PHYSICAL REVIEW D
PARTICLES AND FIELDS

THIRD SERIES, VOLUME 44, NUMBER 1 1 JULY 1991

RAPID COMMUNICATIONS

Rapid Communications are intended for important new results which deserve accelerated publication, and are therefore given priority in editorial processing and production. A Rapid Communication in **Physical Review D** *should be no longer than five printed pages and must be accompanied by an abstract. Page proofs are sent to authors, but because of the accelerated schedule, publication is generally not delayed for receipt of corrections unless requested by the author.*

Higher-statistics measurement of the branching ratio for the decay $K_L^0 \rightarrow \mu\mu$

A. P. Heinson, J. Horvath, C. Mathiazhagan, and W. R. Molzon
University of California, Irvine, California 92717

K. Arisaka, R. D. Cousins, T. Kaarsberg,[a] J. Konigsberg,[b] P. Rubin,[c] W. E. Slater, and D. L. Wagner
University of California, Los Angeles, California 90024

W. W. Kinnison, D. M. Lee, R. J. McKee, E. C. Milner,[d] G. H. Sanders, and H. J. Ziock
Los Alamos National Laboratory, Los Alamos, New Mexico 87545

P. Knibbe[e] and J. Urheim[f]
University of Pennsylvania, Philadelphia, Pennsylvania 19104

K. A. Biery, M. V. Diwan, G. M. Irwin, K. Lang, J. Margulies,[g] D. A. Ouimette, A. Schwartz, and S. G. Wojcicki
Stanford University, Stanford, California 94309

L. B. Auerbach, J. Belz, P. Buchholz,[h] V. L. Highland, W. K. McFarlane,[d] and M. Sivertz[i]
Temple University, Philadelphia, Pennsylvania 19122

J. L. Ritchie and A. Yamashita
University of Texas, Austin, Texas 78712

M. D. Chapman, M. Eckhause, J. F. Ginkel,[j] A. D. Hancock, J. R. Kane, C. J. Kenney,[k] Y. Kuang, W. F. Vulcan, R. E. Welsh, R. J. Whyley,[l] and R. G. Winter
College of William and Mary, Williamsburg, Virginia 23185

(Received 28 February 1991)

With a significant increase in experimental sensitivity, we have observed an additional 281 $K_L^0 \rightarrow \mu\mu$ events after a background subtraction of 19 ± 6 events. Normalizing this sample to the simultaneous observation of the decay $K_L^0 \rightarrow \pi^+\pi^-$, we obtain the branching ratio $B(K_L^0 \rightarrow \mu\mu) = [7.6 \pm 0.5(\text{stat}) \pm 0.4(\text{syst})] \times 10^{-9}$. Combining these data with our previously published sample containing 87 events yields $B(K_L^0 \rightarrow \mu\mu) = (7.0 \pm 0.5) \times 10^{-9}$.

As one of the few measured processes exhibiting an effective flavor-changing neutral current (FCNC), the decay $K_L^0 \rightarrow \mu\mu$ has figured prominently in the development of our understanding of the weak interaction, in particular the Glashow-Iliopoulos-Maiani mechanism [1]. Recent theoretical work has emphasized how precise measurements of this decay rate might restrict the parameters of virtual particles in the decay diagram, most notably those of the top quark. We have reported [2] our earlier measurement of the branching ratio $B(K_L^0 \rightarrow \mu\mu) = [5.8 \pm 0.6(\text{stat}) \pm 0.4(\text{syst})] \times 10^{-9}$. Another recent experiment [3], at KEK, has found $B(K_L^0 \rightarrow \mu\mu) = [8.4$

$\pm 1.1(\text{stat only})] \times 10^{-9}$. In this paper, we report a further measurement of the same quantity using a separate data set with significantly greater statistics, as well as the result for the combined data sets. We collected the new data concurrently with our continuing search for the decay $K_L^0 \rightarrow \mu e$ at the Brookhaven Alternating Gradient Synchrotron (AGS).

The imaginary part of the amplitude for $K_L^0 \rightarrow \mu\mu$ is dominated by the two-photon intermediate state, which has been considered carefully in past years [4]. If the decay were due entirely to this long-distance contribution, the branching ratio would be expected to be $B(K_L^0 \rightarrow \mu\mu) \approx 1.20 \times 10^{-5} \times B(K_L^0 \rightarrow \gamma\gamma) \approx 6.8 \times 10^{-9}$. The strong theoretical expectation is that the introduction of other amplitudes does not appreciably reduce this rate, known as the unitarity bound.

Short-distance diagrams contributing to the real part of the amplitude are calculable [5,6] in the standard model, and become larger as the top-quark mass increases. As precise measurements of the $K_L^0 \rightarrow \mu\mu$ rate constrain the size of the real part of the amplitude, under reasonable assumptions they also constrain the top-quark mass or its couplings [6].

The layout of the experiment, shown in Fig. 1, is optimized for the detection of two-body decays of the K_L^0, namely, those to $\pi^+\pi^-$, $\mu\mu$, μe, or ee. It is well suited to the measurement of the ratio $\Gamma(K_L^0 \rightarrow \mu\mu)/\Gamma(K_L^0 \rightarrow \pi^+\pi^-)$ because the ratio of the raw counting rates for these two similar modes is subject to only minor (near unity) corrections for the differences in the response of the apparatus to them. As described in more detail in previous publications [2,7], 24-GeV/c protons impinging on a copper target created the secondary beam, which was collimated and swept free of charged particles in the 9.5 m following the target. The resulting neutral beam had an angular divergence of 4.1 mrad horizontally by 15 mrad vertically, and contained neutrons and kaons in the ratio of (18 ± 6):1 as determined by beam studies. The neutral particles traveled through an evacuated decay region (< 0.02 Torr) of 8.5 m length which terminated in a vacuum window, which was followed by helium bags.

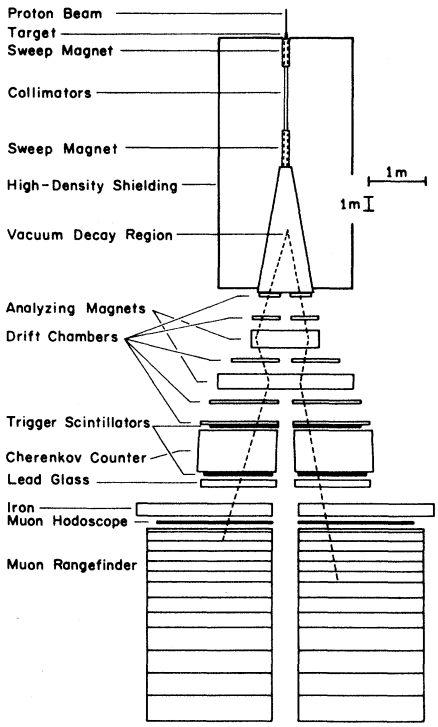

FIG. 1. Plan view of the apparatus.

The accepted decay products of kaons decaying in the vacuum region emerged through separate windows and traversed independent spectrometer arms on either side of the neutral beam. Each spectrometer arm contained five drift-chamber modules interspersed among two analyzing magnets which permitted redundant measurements of each track's momentum. Each module consisted of two x- and two y-measuring planes, each with local position resolution of 120 μm. (In the coordinate system referred to, $+y$ is up, $+x$ is to beam left, and $+z$ is the nominal neutral beam direction.) The regions between the chambers were occupied by thin-walled helium bags to reduce multiple scattering and nuclear interactions.

Following the last drift chamber in each detector arm were, in sequence, an x-y array of finely segmented scintillation trigger counters, a threshold gas Cerenkov counter, another trigger counter array, a lead-glass array which included more scintillation counters, and then a 91-cm-thick iron wall to filter out (together with the lead glass) all particles except muons above a momentum of about 1.4 GeV/c. Finally, there were two muon detection systems which were important for this analysis. The position and time were measured using the muon hodoscope consisting of segmented x- and y-measuring scintillation counters. Muons then lost energy and, in most cases of interest, stopped in the range finder [8] consisting of vertical slabs of marble and aluminum. At thirteen z positions corresponding to 10% momentum increments, there were planes of x-y proportional tubes to measure the range of the muons.

The level-1 minimum-bias trigger for two-track events required a coincidence of signals from the first three drift-chamber modules and the upstream and downstream trigger counter hodoscopes in both detector arms. The $K_L^0 \rightarrow \pi^+\pi^-$ normalization events, as well as some K_{l3} events ($K_L^0 \rightarrow \pi e \nu$ and $K_L^0 \rightarrow \pi\mu\nu$) needed for studies, were in a sample of minimum-bias events prescaled in hardware by 2000, and further prescaled off line by 3. The level-1 $K_L^0 \rightarrow \mu\mu$ trigger was the minimum-bias trigger in further coincidence with the muon hodoscopes on each side.

After each level-1 trigger, flash time-to-digital converters, analog-to-digital converters, and latches digitized [9] the detector signals within 200 ns. Each event was read out [10] into one of eight 3081/E processors [11] where partial track reconstruction (using only the first three drift-chamber modules) and event analysis were performed. The processors calculated the two-body invariant masses m_{12} ($m_{\mu\mu}$ and $m_{\pi\pi}$, as appropriate) and the collinearity angle θ_K, defined to be the angle between the two-track three-momentum sum and the line from the tar-

get to the reconstructed kaon decay vertex. $K_L^0 \to \mu\mu$ candidates were filtered by cuts on these quantities in the processors and by tighter cuts on the same quantities off line, while the $K_L^0 \to \pi^+\pi^-$ candidates were cut only off line on the same quantities (thus allowing off-line monitoring of these calculations and cuts). The net requirements for both decays were $460 \leq m_{12} \leq 550$ MeV/c^2 and $\theta_K \leq 10$ mrad. Although these cuts were not tight compared to the resolution in these quantities, the efficiency of the off-line cut on $K_L^0 \to \pi^+\pi^-$ events passing all other final analysis cuts was only 64.1%, mainly due to pattern recognition difficulties stemming from the high rate of the first three chamber modules. Detailed off-line studies of possible differences between $K_L^0 \to \pi^+\pi^-$ and $K_L^0 \to \mu\mu$ events confirmed that the ratio of efficiencies of these two cuts for the two modes was 1.00 ± 0.01, as expected for two such kinematically similar decay modes.

In the off-line analysis, the track-finding algorithm used hits in the trigger scintillation counters and all drift chambers to reconstruct tracks and the decay vertex. The algorithm allowed up to two hits to be missing in each view of each track. The masses and collinearity angles were recalculated using the off-line tracks and an approximate momentum analysis, and further cuts applied: $470 \leq m_{12} \leq 530$ MeV/c^2 and $\theta_K \leq 3.16$ mrad.

Two different methods were then used to fit the track hits using the full magnetic-field maps, recalculating the choice of left-right ambiguity solution as necessary. The first method calculated track orbits and momenta in the upstream (front) and downstream (back) magnets separately, and computed track χ^2 quantities [2,7] based on the consistency of these results and their matching at the third drift-chamber module. The second method fit the hits in an entire spectrometer arm to a single track orbit. In doing this, it minimized a χ^2 which accounted for the expected correlations, due to multiple scattering, in departures of hits from ideal track orbits. It also calculated momenta and orbits using each magnet separately, similar to the first method. Both methods also constructed and cut loosely on an additional χ^2 associated with the quality of the two-track vertex. We carried out the full analysis using each fitting method separately. As the results had negligible differences, we present here only the results using the second method.

Since the track χ^2 distributions for both methods showed some disagreement between data and Monte Carlo simulation, the cuts on these quantities were kept relatively loose. Studies of pion and muon tracks from K_{l3} decays established that the relative loss of $K_L^0 \to \pi^+\pi^-$ and $K_L^0 \to \mu\mu$ decays associated with our uncertain understanding of the χ^2 distribution leads to a systematic uncertainty in the ratio of rates of less than 2%. To compensate for the loose χ^2 cuts, we required that the momentum measured with the front magnet (p_{front}) and momentum measured with the back magnet (p_{back}) be close enough such that $(p_{\text{back}} - p_{\text{front}})/[(p_{\text{back}} + p_{\text{front}})/2] \leq 0.05$. The distribution in this quantity is shown in Fig. 2 for each data set with all other cuts imposed. The rms deviation of a Gaussian distribution fit to the pion data is 0.0094. As a function of track momentum, the fit Gaussian rms deviation ranges from 0.0081 at 2 GeV/c to 0.011 at 6 GeV/c.

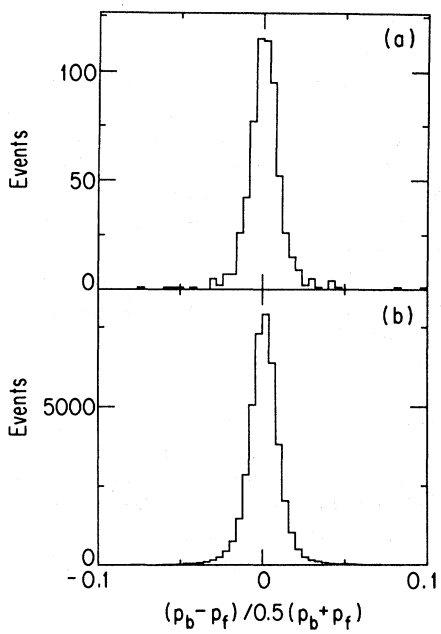

FIG. 2. The relative back-front momentum difference $(p_{\text{back}} - p_{\text{front}})/[(p_{\text{back}} + p_{\text{front}})/2]$, after all other cuts are made, for (a) $K_L^0 \to \mu\mu$ candidates and (b) $K_L^0 \to \pi^+\pi^-$ candidates.

To identify muons in the muon hodoscope, we required consistency between the positions of the struck counters and the positions expected from projections of the reconstructed track orbits, between the times in the x- and y-measuring counters, and between the muon-hodoscope time and an event time determined by the trigger scintillators. These requirements were implemented by a single cut on an overall muon-hodoscope confidence level which included the momentum dependence of the distributions of these differences.

The range-finder analysis employed a track-following algorithm which found the deepest (most downstream) of the series of struck proportional tubes consistent with the candidate muon track. We required that the plane number (1–13) of the deepest associated struck tube minus the plane number of the expected deepest tube (based on the spectrometer momentum measurement) be greater than or equal to -3.

The single-track efficiencies of the muon-hodoscope and range-finder cuts were tabulated individually with samples of minimum-bias tracks from $K_{\mu 3}$ decays, as a function of track momentum and, where appropriate, position. The overall efficiency for a $K_L^0 \to \mu\mu$ event to pass all off-line muon identification cuts on both tracks was determined to be 0.929 ± 0.015 by appropriately weighting Monte Carlo $K_L^0 \to \mu\mu$ events by the probability that the tracks passed the cuts. The two detectors contributed factors of approximately 0.95 and 0.98, respectively. In addition, the probability that an event satisfied the level-1 hardware $\mu\mu$ trigger, given that it passed off-line muon cuts, was measured to be 0.984 ± 0.002 using a large sample of $K_{\mu 3}$ events (from minimum bias triggers) where the pion decayed to a second muon. The total probability $\epsilon_{\mu\mu}$ that a $K_L^0 \to \mu\mu$ event satisfied trigger and off-line muon

identification criteria was thus 0.914 ± 0.015.

We made additional cuts, with little loss, to ensure that events were contained in the vacuum decay volume and detector. Events with reconstructed vertex $z < 9.75$ m were eliminated to reject backgrounds from decays within the field of the last sweeping magnet and particles from interactions with the collimators. We also eliminated events with tracks that passed too close to magnet iron or the vacuum window flange. Tracks were also required to be above 1.5 GeV/c to eliminate kinematic regions with very low acceptance. Because of the kinematic similarity of $K_L^0 \to \mu\mu$ and $K_L^0 \to \pi^+\pi^-$ decays, the effect of these additional cuts on the relative efficiency was negligible ($< 0.5\%$).

Figure 3(a) is a scatter plot of θ_K^2 vs $m_{\mu\mu}$ for events passing all the selection criteria. There are 300 events (including background) in the signal region: $|m_{\mu\mu} - m_{K_L}| \leq 6$ MeV/c^2 and $\theta_K^2 \leq 2\times10^{-6}$. Figure 3(b) is the projection onto the mass axis of events with $\theta_K^2 \leq 2\times10^{-6}$. We have estimated the background by studying various regions of the scatter plot, in particular the region in the same mass window but with $\theta_K^2 > 2.0\times10^{-6}$, and with muon identification cuts varied. These events are nearly uniformly distributed in θ_K^2, with a departure from uniformity consistent with Monte Carlo simulations of the decay $K_L^0 \to \pi e \nu$ where both particles are misidentified as muons. (Most of these events have signals in the electron-identifying detectors which were not used in this analysis.) Extrapolating into the signal region from 14 events with $2.0\times10^{-6} < \theta_K^2 < 4.0\times10^{-6}$, we estimate 19 ± 6 background events. Hence the number of signal events is $N_{\mu\mu} = 281 \pm 18$.

The $K_L^0 \to \pi^+\pi^-$ normalization events are selected with identical cuts except that no particle-identification cuts are made. As a consequence, there is background on the plot of $m_{\pi\pi}$ for these events, shown in Fig. 4. The shape of this background is reproduced well by a Monte Carlo simulation of K_{l3} events where both particles are analyzed as pions. We adjust the scale of the background curve to obtain agreement with the data on the number of events outside the $K_L^0 \to \pi^+\pi^-$ signal region (events with $475 \leq m_{\pi\pi} < 488$ MeV/c^2 plus events with $508 \leq m_{\pi\pi} < 525$ MeV/c^2), and then use it to estimate the number of background events under the peak. The result is $N_{\pi\pi} = 15795 \pm 167$ events, where the uncertainty includes contributions from the background subtraction and statistical fluctuation of the signal. $N_{\pi\pi}$ includes the small effect of event-by-event weights which account for the probability that the parent neutral kaon was a K_L^0 (as a function of proper time of decay). (For high-momentum kaons which decay at low z, there is some contamination from the K_S^0 and interference terms in the state function.) The net effect of these weights is to lower the value of $N_{\pi\pi}$ by 1.6% from the unweighted value to the value above.

The adjustment in the scale of the background simulation in Fig. 4 results in a difference of only 4% from the expectation based on known branching ratios of K_{l3} and $K_L^0 \to \pi^+\pi^-$ decays, providing a consistency check of our normalization. As a further check of our methods, including muon identification, we have measured the rate of $K_{\mu3}$ vs $K_L^0 \to \pi^+\pi^-$ over a wider range of mass and collinearity, and find a value only 2% higher than the Particle Data Group [12] average.

We compute the branching ratio for $K_L^0 \to \mu\mu$ from the world-average branching ratio [12] for $K_L^0 \to \pi^+\pi^-$ [$(2.03 \pm 0.04)\times10^{-3}$] and our result for $N_{\mu\mu}/N_{\pi\pi}$, corrected for differences between the decays:

$$B(K_L^0 \to \mu\mu) = B(K_L^0 \to \pi^+\pi^-) \frac{N_{\mu\mu}}{6000 \times N_{\pi\pi}} \frac{A_{\pi\pi}}{A_{\mu\mu}} \frac{\epsilon_{\pi\pi}}{\epsilon_{\mu\mu}},$$

where 6000 is the net prescale factor for minimum-bias events, and $A_{\pi\pi}/A_{\mu\mu} = 1.185 \pm 0.013$ is the relative acceptance of $\pi\pi$ and $\mu\mu$ events as determined by Monte Carlo simulation with full event reconstruction. The acceptances for $K_L^0 \to \mu\mu$ and $K_L^0 \to \pi^+\pi^-$ decays differ due to the difference in Q value and the decays of some of the

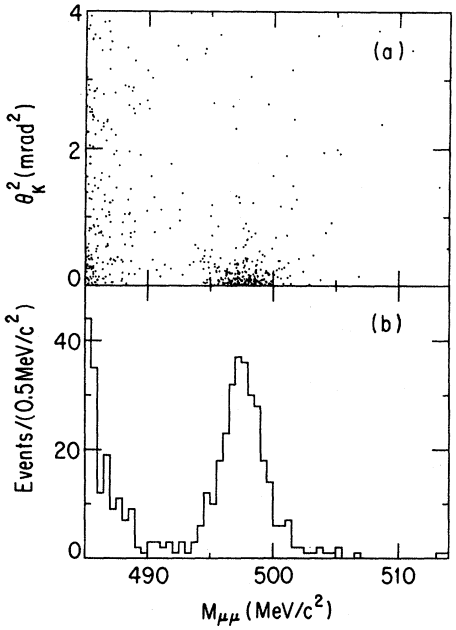

FIG. 3. For the final $K_L^0 \to \mu\mu$ candidate sample, (a) scatter plot of θ_K^2 vs $m_{\mu\mu}$ and (b) histogram of $m_{\mu\mu}$ for events with $\theta_K^2 \leq 2\times10^{-6}$.

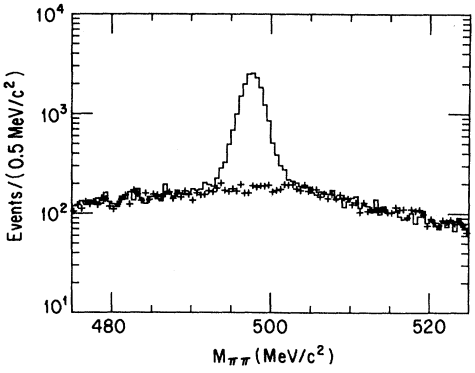

FIG. 4. The $m_{\pi\pi}$ spectrum for events in the final-event sample with $\theta_K^2 \leq 2\times10^{-6}$. The line is the prescaled minimum-bias data and the points are the Monte Carlo simulation of the background.

pions. The factor $\epsilon_{\pi\pi}$ accounts for the loss of $K_L^0 \to \pi^+\pi^-$ events due to pion-nucleon interactions in the spectrometer, estimated to be 0.97 ± 0.01. Combining the above numbers yields

$$B(K_L^0 \to \mu^+\mu^-) = (7.6 \pm 0.5 \pm 0.4) \times 10^{-9}.$$

The errors are statistical and systematic, respectively. The systematic error includes the effect of changes in the result due to reasonable variations in all cuts.

While this result is somewhat higher than the value computed from our previous data set [2], we have found no significant corrections to the previous analysis. We combine the results from the two data sets by constructing a likelihood function for each data set, and maximizing the product of the two likelihood functions. In constructing the likelihood function for each data set, we assume Poisson probability functions for the number of $K_L^0 \to \mu\mu$ events and Gaussian probability density functions for systematic uncertainties. Correlated uncertainties (such as the $K_L^0 \to \pi^+\pi^-$ branching ratio) are withheld from the likelihood functions and added in quadrature to the uncertainties obtained from the likelihood method. We obtain

$$B(K_L^0 \to \mu^+\mu^-) = (7.0 \pm 0.5) \times 10^{-9}$$

as the combined result from our two data sets. The uncertainty contains the combined effects of statistical and systematic uncertainties, which are approximately 0.4×10^{-9} and 0.3×10^{-9}, respectively. Our central value for $B(K_L^0 \to \mu^+\mu^-)$ is less than one-half standard deviation above the unitarity bound.

We thank the AGS staff, particularly H. Brown, J. W. Glenn, and J. Mills, for their support. We also thank J. Cook, G. Daniel, G. Hart, V. Hart, J. Kubic, F. Mansell, C. Pierce, M. Roehrig, A. Tilghman, and Q. Trang for their technical assistance. We also thank the BNL Computing and Communications Division and the Cornell National Supercomputer Facility for timely processing of a large volume of data. S. Axelrod, G. Bonneaud, J. Frank, J. Greenhalgh, P. Guss, J. Martoff, P. Melese, and W. Wales made valuable contributions to the first stages of this work. This research is supported by the U.S. Department of Energy and the National Science Foundation.

---

[a]Present address: American Physical Society, Washington, DC 20009.
[b]Present address: Harvard University, Cambridge, MA 02138.
[c]Present address: Syracuse University, Syracuse, NY 13244.
[d]Present address: Superconducting Super Collider Laboratory, Dallas, TX 75237.
[e]Present address: Intermetrics Inc., Warminster, PA 18974.
[f]Present address: California Institute of Technology, Pasadena, CA 91125.
[g]Present address: Los Alamos National Laboratory, Los Alamos, NM 87545.
[h]Present address: CERN, CH-1211 Geneva 23, Switzerland.
[i]Present address: University of California, San Diego, La Jolla, CA 92093.
[j]Present address: University of Colorado, Boulder, CO 80309.
[k]Present address: Stanford Linear Accelerator Center, Stanford, CA 94309.
[l]Present address: MCI Communications Corp., McLean, VA 22102.

[1] S. Glashow, J. Iliopoulos, and L. Maiani, Phys. Rev. D **2**, 1258 (1970).
[2] C. Mathiazhagan *et al.*, Phys. Rev. Lett. **63**, 2185 (1989).
[3] T. Inagaki *et al.*, Phys. Rev. D **40**, 1712 (1989).
[4] L. M. Sehgal, Phys. Rev. **183**, 1511 (1969); B. R. Martin, E. de Rafael, and J. Smith, Phys. Rev. D **2**, 179 (1970); H. Stern and M. Gaillard, Ann. Phys. (N.Y.) **76**, 580 (1973).
[5] M. Gaillard and B. Lee, Phys. Rev. D **10**, 897 (1974); M. K. Gaillard, B. W. Lee, and R. E. Schrock, *ibid.* **13**, 2674 (1976).
[6] R. E. Shrock and M. B. Voloshin, Phys. Lett. **87B**, 375 (1979); T. Inami and C. S. Lim, Prog. Theor. Phys. **65**, 297 (1981); L. Bergstrom, E. Masso, P. Singer, and D. Wyler, Phys. Lett. **134B**, 373 (1984); N. F. Nasrallah and K. Schilcher, Z. Phys. C **36**, 467 (1987); F. Gilman, in *Physics at the 100 GeV Mass Scale,* Proceedings of the 17th SLAC Summer Institute, Stanford, California, 1989, edited by E. C. Brennan (SLAC Report No. 361, Stanford, 1990), p. 483; C. S. Kim, J. Rosner, and C.-P. Yuan, Phys. Rev. D **42**, 96 (1990); C. Geng and J. Ng, Phys. Rev. D **41**, 2351 (1990); L. Bergstrom, E. Masso, and P. Singer, Phys. Lett. B **249**, 141 (1990); G. Belanger and C. Geng, Phys. Rev. D **43**, 140 (1991).
[7] C. Mathiazhagan *et al.*, Phys. Rev. Lett. **63**, 2181 (1989).
[8] J. Frank *et al.*, IEEE Trans. Nucl. Sci. **36**, 79 (1989); C. J. Kenney *et al.*, *ibid.* **36**, 74 (1989); D. M. Lee *et al.*, Nucl. Instrum. Methods Phys. Res. Sect. A **256**, 329 (1987).
[9] R. D. Cousins *et al.*, IEEE Trans. Nucl. Sci. **36**, 646 (1989); K. A. Biery *et al.*, *ibid.* **36**, 650 (1989).
[10] R. D. Cousins *et al.*, Nucl. Instrum. Methods Phys. Res. Sect. A **277**, 517 (1989).
[11] P. F. Kunz *et al.*, Report No. SLAC-PUB-3332, 1984 (unpublished).
[12] Particle Data Group, J. J. Hernandez *et al.*, Phys. Lett B **239**, 1 (1990).